

BARBARA LARWA, KRZYSZTOF KUPIEC, TADEUSZ KOMOROWICZ,
KRZYSZTOF NEUPAUER*

HEAT CONDUCTION IN THE GROUND UNDER NATURAL CONDITIONS AND WITH HEAT EXCHANGER INSTALLED

PRZEWODZENIE CIEPŁA W GRUNCIE W WARUNKACH NATURALNYCH I PRZY ZAINSTALOWANYM WYMIENNIKU CIEPŁA

Abstract

The results of calculations of the heat transfer in a horizontal ground heat exchanger are presented. The applied model is based on a one-dimensional equation of the transient heat conduction with an internal heat source. The model was correctly verified by comparison of computational results and experimental measurements presented in literature. Thermal calculations concerning heat transfer in the ground under natural conditions are also presented.

Keywords: horizontal ground heat exchangers, transient heat conduction

Streszczenie

Przedstawiono wyniki obliczeń przenoszenia ciepła w poziomym gruntowym wymienniku. Model użyty w obliczeniach oparto na jednowymiarowym równaniu nieustalonego przewodzenia ciepła z wewnętrznym źródłem. Model został zweryfikowany przez porównanie wyników obliczeń z wynikami pomiarów przedstawionymi w literaturze. Przeprowadzono również obliczenia dotyczące przenoszenia ciepła w gruncie w warunkach naturalnych.

Słowa kluczowe: poziome gruntowe wymienniki ciepła, nieustalone przewodzenie ciepła

DOI: 10.4467/2353737XCT.15.105.4053

* M.Sc. Eng. Barbara Larwa, Ph.D. D.Sc. Eng. Krzysztof Kupiec, prof. CUT, Ph.D. Eng. Tadeusz Komorowicz, PhD. Eng. Krzysztof Neupauer, Department of Chemical and Process Engineering, Faculty of Chemical Engineering and Technology, Cracow University of Technology.

Nomenclature

$a (= k/(c\rho))$	– thermal diffusivity of the ground [m^2/s]
A_g	– surface area of the ground [m^2]
B	– half of the annual maximum temperature range [K]
Bi	– Biot number
C_1, C_2	– constants dependent on the Biot number
c	– heat capacity of the ground [$\text{J}/(\text{kgK})$]
F	– heat flux [W/m^2]
h	– distance between the heat exchanger and the ground surface [m]
h_0	– heat transfer coefficient [$\text{W}/(\text{m}^2\text{K})$]
k	– thermal conductivity of the ground [$\text{W}/(\text{mK})$]
L	– characteristic length [m]
m	– number of stages
\dot{m}	– mass flow rate [kg/s]
q	– total amount of heat per unit area of the ground [J/m^2]
q_v	– rate of heat generation per unit of volume [W/m^3]
\dot{Q}	– rate of heat transfer [W]
t	– time [days]
t_c	– cycle time [days]
t_{\max}	– time from the beginning of the year until the maximum ambient temperature is reached [days]
T	– temperature [$^{\circ}\text{C}$]
T_b	– temperature of the ground at great depth [$^{\circ}\text{C}$]
x	– position coordinate [m]
ρ	– ground density [kg/m^3]
ω	– frequency [1/s]

Indices

0	– ground surface
a	– ambient (environment)
g	– ground
L	– working fluid
-	– average value

1. Introduction

The ground is an advantageous heat source for heat pumps. Compared to air, the ground has a much more stable temperature and a high specific heat.

The heat is transported between a ground surface and the environment (atmospheric air). The direction of heat transfer depends on the relation between the ground temperature and the ambient temperature. In the warmer half of the year, the air temperature is higher than the ground temperature; inversely in the cooler half of the year. The greater the temperature difference between the ground surface and the environment, the greater the heat flux transferred.

Cyclicity of the air temperature changes cause the temperature of the ground below a certain depth (about 10 m) to be equal to the average ambient air temperature. On the other hand, the temperature of the sub-surface of the ground varies both with time as well as with the position (depth). The installation of a ground heat exchanger at the shallow depth of the ground (embedded horizontally) along with receiving or transferring the heat with its utilization disrupts the natural cycle of ground temperature changes. During receiving of the heat from the ground in heating season, the ground temperature lowers. Due to the small installation depth of a horizontal heat exchanger, those temperature changes also apply to the ground surface. The cooling of the ground surface causes an increase in the temperature difference between the air and ground surface and thus the ground then takes more heat than it does under natural conditions. Vertical exchangers do not have this beneficial feature as the cold ground at great depth is not able to compensate the heat loss by receiving heat from the environment.

Horizontal ground heat exchangers have been widely used in many countries as a heat source for ground-source heat pump systems. Therefore, ground heat exchangers are a subject of many experimental and numerical studies [1–6].

The subject of this paper is to present the results of thermal calculations concerning horizontal ground heat exchangers. The calculations were performed on the basis of the solution of equations of the mathematical model of the process. The ground was considered as a semi-infinite body with an internal heat source, wherein, it has been taken into account that atmospheric air has a temperature changing periodically in time. The presented results can be used to simulate ground heat exchangers under different conditions.

2. Analytical solutions of transient heat conduction in the ground

The sub-surface of the ground was considered as a semi-infinite body limited from the top by the ground surface. The heat conduction equation has the form:

$$\frac{\partial T}{\partial t} = a \frac{\partial^2 T}{\partial x^2} + \frac{q_v}{c\rho} \quad (1)$$

If the ground heat exchanger is not installed $q_v = 0$.

It was assumed that the heat between the ground and the environment is transferred by convection; the boundary condition for the surface of the ground is as follows:

$$x = 0 \quad L \frac{\partial T}{\partial x} = -\text{Bi}(T_a - T) \quad (2)$$

where Bi is the Biot number characterizing the ratio between the internal and external resistances to heat transfer, defined as follows:

$$\text{Bi} = \frac{h_0 L}{k} \quad (3)$$

The quantity L (with length dimension) is defined as below:

$$L = \sqrt{\frac{2a}{\omega}} \quad (4)$$

A boundary condition relates to the ground at a great depth where the temperature is constant. The condition is following:

$$x \rightarrow \infty \quad T = T_b \quad (5)$$

The ambient temperature T_a changes periodically according to the relationship:

$$T_a = \bar{T}_a + B \cdot \cos [\omega(t - t_{\max})] \quad (6)$$

wherein the values \bar{T}_a and T_b are the same. A frequency ω is equal to:

$$\omega = \frac{2\pi}{t_c} \quad (7)$$

where t_c is the cycle time (365 days). For a cyclic steady state the equation (1) with combination with (2), (5) and (6) has an analytical solution. The relationship of the ground temperature in the function of the time and position has the form [7]:

$$T = T_b + BC_1 \cdot \exp\left(-\frac{x}{L}\right) \cdot \cos\left[\omega(t - t_{\max}) - \frac{x}{L} - C_2\right] \quad (8)$$

where C_1 and C_2 depend on the Biot number:

$$C_1 = \frac{\text{Bi}}{\sqrt{(\text{Bi} + 1)^2 + 1}} \quad (9)$$

$$C_2 = \tan^{-1}\left(\frac{1}{\text{Bi} + 1}\right) \quad (10)$$

In Figs. 1a and b, the temperature profiles in the ground, determined according to relationship (8), are presented. The ground temperature profiles are shown in 3-month intervals (January, April, July, October). The calculations were performed for $\text{Bi} = 2$ and $\text{Bi} \rightarrow \infty$. As one can see from the Figs. 1a and b for $x/L > 5$, the temperatures change slightly. In addition, for smaller values of Bi the temporal variations of temperatures in the sub-surface layers of the ground become less significant.

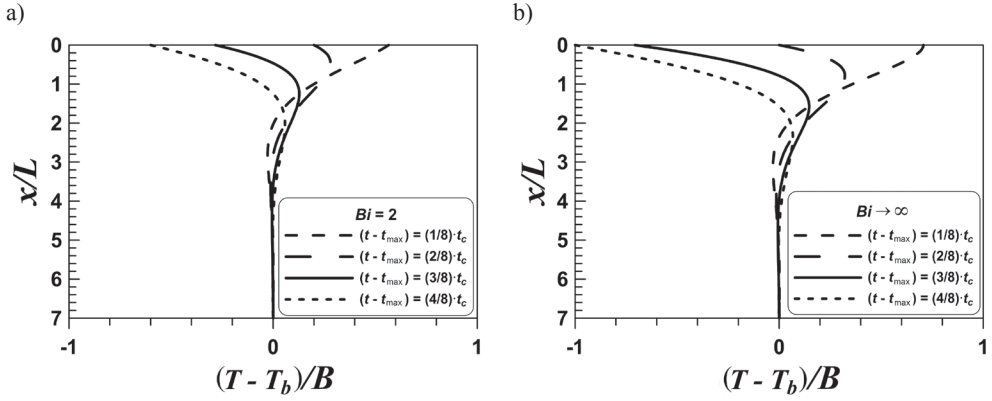


Fig. 1. Ground temperature profiles for a) $Bi = 2$, b) $Bi \rightarrow \infty$

The temperature gradient on the ground surface can be obtained by differentiation of formula (8):

$$L \left(\frac{\partial T}{\partial x} \right)_{x=0} = -\sqrt{2} BC_1 \cdot \cos \left[\omega(t - t_{\max}) - C_2 + \frac{\pi}{4} \right] \quad (11)$$

The heat flux on the surface of the ground, in accordance with the Fourier equation, is:

$$F = -k \left(\frac{\partial T}{\partial x} \right)_{x=0} \quad (12)$$

This flux can be determined by calculation of the temperature gradient at the ground surface. One gets:

$$F = \sqrt{2} \frac{kBC_1}{L} \cdot \cos \left[\omega(t - t_{\max}) - C_2 + \frac{\pi}{4} \right] \quad (13)$$

The maximum heat flux is as follows:

$$F_{\max} = \sqrt{2} \frac{kBC_1}{L} \quad (14)$$

The time, after the heat flux reaches the maximum value is following:

$$t = t_{\max} + t_c \left(\frac{C_2}{2\pi} - \frac{1}{8} \right) \quad (15)$$

For a time higher by $t_c/2$ than the time specified above (i.e. after a half-year period), the heat flux reaches the value according to the formula (14), but with the opposite sign (minimum function) – this applies to the transport of heat from the ground to the environment.

Temporal changes in the heat flux between the ground and the environment can be determined from relationship (13) and are shown in Fig. 2. The effect of the Biot number, inversely proportional to the external thermal resistance, was analyzed. The greater the external thermal resistance, the smaller the heat flux between the ground and the environment for certain values of B , k and L . The value of the external thermal resistance affects not only the heat flux, but also the date of occurrence of the maximum flux. For $B = 11$ K, $k = 1.5$ W/(mK), $L = 2.24$ m and $t_{\max} = 182$ days (the warmest day in the year – 1st of July) exemplary values can be read from the graph. If the external thermal resistance can be neglected, the maximum heat flux $F_{\max} = 9.5$ W/m² ($F_{\max} L/(kB) = 1.41$) is reached on the 14th of May. This date is 46 days before the warmest day of the year, while for $Bi = 2$ the maximum value of heat flux is $F_{\max} = 6.6$ W/m² ($F_{\max} L/(kB) = 0.89$) and it is reached 24 days later.

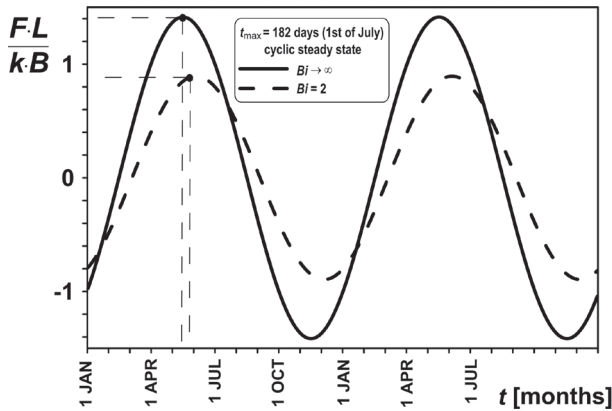


Fig. 2. Temporal variation of heat flux to/from the ground surface

The integration of the heat flux over time leads to the determination of the amount of heat q transported to/from the ground per unit area. The limits of integration for heating the ground (including the half-year period) result from the condition $(\partial T/\partial x)_{x=0} < 0$. Therefore, the values of the cosine function (13) are positive. In the next half-year period, the temperature gradient at the surface of the ground is positive, the values of cosine function are negative and the ground transfers the heat to the environment ($q < 0$). The resulting lower limit of integration (when the ground is heated) is $t_{\max} + (C_2 - 3\pi/4)/\omega$ and the upper is $t_{\max} + (C_2 + \pi/4)/\omega$. As a result of integration one gets:

$$q = \int_{t_{\max} + (C_2 - 3\pi/4)/\omega}^{t_{\max} + (C_2 + \pi/4)/\omega} F \cdot dt = 2BC_1D \quad (16)$$

where:

$$D = \sqrt{\frac{kcp}{\omega}} \quad (17)$$

Fig. 3 refers to the total amount of heat per unit area of the ground q , for that half of the year when the direction of heat transfer does not change (in the warmer half of the year). The relationship between q and the product (kcp) for various values of B and Bi are presented. The calculations were carried out for $\omega = 0.199 \cdot 10^{-6} \text{ s}^{-1}$. With the increase in the values of (kcp) , B and Bi the amount of heat taken over by the ground during the warmer half of the year increases. Exemplary for $B = 11 \text{ K}$, $k = 1.5 \text{ W/(mK)}$, $c\rho = 6.5 \text{ MJ/(m}^3\text{K)}$ and $Bi = 2$ one obtains $q = 97.4 \text{ MJ/m}^2$, whereas for $Bi \rightarrow \infty$ a higher value is obtained: $q = 158 \text{ MJ/m}^2$.

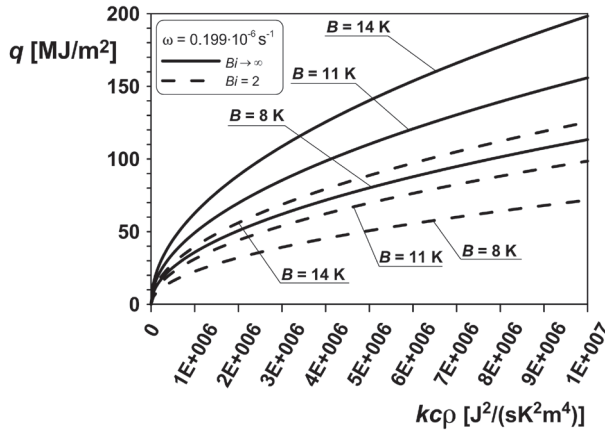


Fig. 3. The effect of product (kcp) , B and Bi on the amount of heat taken over by the ground

By knowing the temperature profiles in the ground, one can determine the average temperature of the sub-surface layer of the ground. This quantity has an apparent sense because its value depends on the depth of the ground layer which is considered to be the sub-surface layer (below the sub-surface layer the ground has a temperature approximately independent of the time and position). It is assumed in calculations that the thickness of the sub-surface layer is 2π -fold higher than the characteristic linear dimension. The average temperature of the sub-surface layer of the ground was calculated according to the formula:

$$\bar{T} = T_b + \frac{1}{2\pi} \int_0^{2\pi} \Delta T dX \quad (18)$$

where: $\Delta T = T - T_b$. Substituting (8) to (18) one gets after integration:

$$\bar{T} = T_b + \frac{BC_1}{4\pi} \left\{ \sin[\omega(t - t_{\max}) - C_2] + \cos[\omega(t - t_{\max}) - C_2] \right\} \quad (19)$$

In Fig. 4, the temporal courses of the average ground temperature throughout the year are shown. Also in this case, there is a major impact of the Biot number on the obtained calculation results. For $Bi \rightarrow \infty$, the lowest ground temperature appears on the 14th of February and the highest – on the 16th of August. For $Bi = 2$ the average temperature reaches the extreme value 18–19 days later.

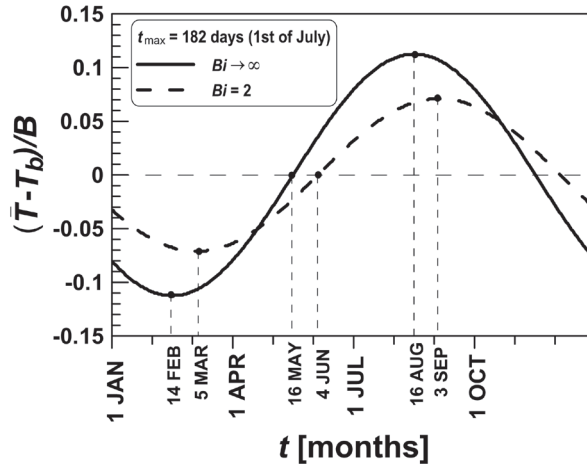


Fig. 4. Courses of average temperature of sub-surface of the ground

In the particular case of absence of the thermal resistance of heat transfer between the surface of the ground and the environment $h_0 \rightarrow \infty$ and $Bi \rightarrow \infty$. Since then $C_1 = 1$ and $C_2 = 0$ and the above relationships simplify.

3. Mathematical model of a horizontal ground heat exchanger

If a heat exchanger is installed in the ground $q_v \neq 0$ and the heat conduction equation (1) with conditions (2), (5) and (6) should be solved numerically.

In the presented model, the flow through parallel arrangement of heat exchanger pipes is replaced by a flow through a horizontal cuboid channel of small thickness. The heat is transferred into (from) the ground symmetrically by both the lower and the upper surface of the heat exchanger.

In Fig. 5, the ground exchanger is shown as a fictitious cuboid, wherein, the heat is generated. Inside a cuboid of dimensions $L_g \times b \times \delta$, the temperature is equalized along the axis x and z at any time. The temperature variation along the y -axis is taken into account

by dividing the heat exchanger into stages. A working fluid flows in series through the neighboring stages, which are treated in the model as perfect-mixing tanks. One of these tanks is shown demonstratively (Fig. 5).

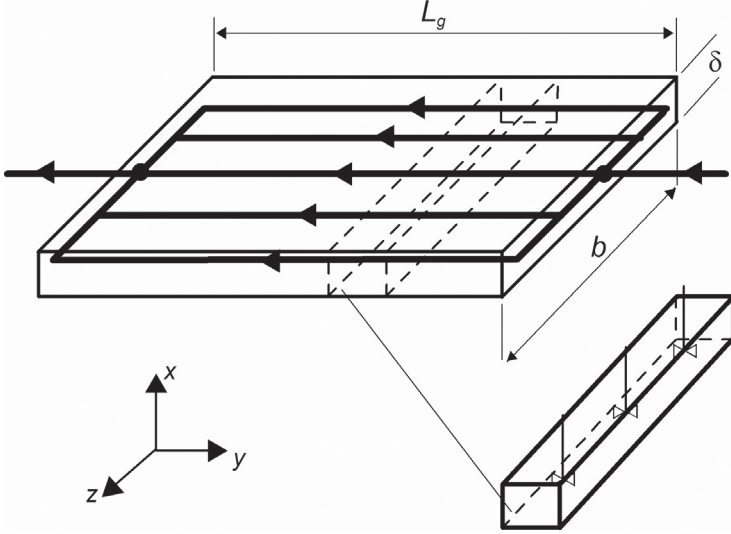


Fig. 5. Ground heat exchanger as a horizontal cuboid channel

In the case of ground heat exchangers, the thermal resistance occurs in working fluid and in walls of pipes but mainly in the ground. Individual resistances are related to areas through which the heat is transported. The presented model only includes the resistance to heat transfer in the ground. The consequence of this is that the surface of the pipes is not used in the model. For the modeled exchanger, it can be assumed that the heat transfer surface is a surface of the ground A_g where the exchanger pipes are installed. The quantity A_g should be treated as an adjustable parameter of the model that depends on the way of arrangement of pipes and the depth of their location under the ground surface.

In this model, the equation for an infinite plate, for which one surface is the surface of ground, and the other is located at a great depth providing the ground temperature stability is used. For transient conduction in an infinite plate with an internal heat source, the relationship (1) is valid; the quantity q_v is a rate of heat generation of the heat source per unit volume:

$$q_v = -\frac{\dot{Q}}{V} \quad (17)$$

where V is the volume of horizontal cuboid. \dot{Q} is related to the transport of heat between the working fluid flowing through the ground heat exchanger and the ground. A detailed description of the model is shown in work [5].

4. Experimental verification of the model

In order to verify the presented mathematical model of the horizontal ground heat exchanger, the ground temperature profiles generated computationally in period of 53 days during the heating season, were compared with the measurement results presented by Wu et al. [6]. The cited authors researched the ground heat exchanger used as a lower heat source of a heat pump for space heating. Horizontal coils of exchanger pipes were arranged in four rows with a width of 1 m and a length of 80 m each, at a depth of 1.14 m. The exchanger operated continuously. Ground temperature was measured at seven depths in the range of 0 to 1.14 m. The measurements were conducted in close proximity to the heat exchanger pipes and, separately, away from any of the heat exchanger pipes (reference hole).

In model calculations it was assumed that the environment temperature periodically varied in time according to the relation:

$$T_a = T_b + B \cdot \cos \left[\omega (t - t_{\max,y}) \right] + B_d \cos \left[\frac{2\pi}{24} (t - t_{\max,d}) \right] \quad (18)$$

where B_d is half of the maximum daily temperature range. In the above formula, the second term applies to temperature variability in the annual cycle (y) and the third term – in the diurnal cycle (d).

The model course of the air temperature under measurements conditions (7th Nov–28th Dec, around London) is presented in Fig. 6.

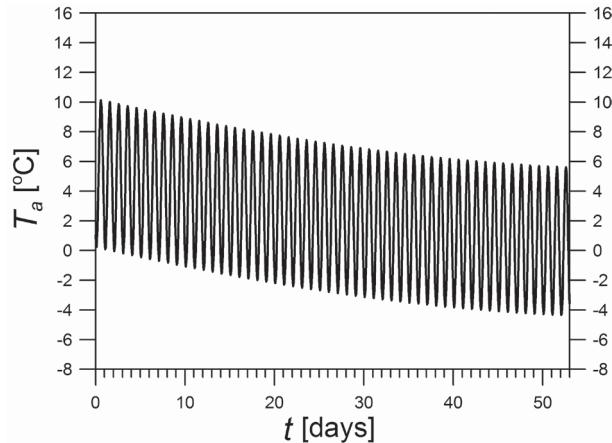


Fig. 6. The air temperature course (Eq. (18))

In the calculations based on the model, the following values of parameters were used: $n = 300$ (number of calculation nodes), time step $\Delta t = 1$ h. The data according to which the calculations were carried out are presented in Table 1.

Table 1

The process parameters used in calculations

Symbol	Value	Symbol	Value
\dot{Q}	4220 [W]	m	4
k	1.24 [W/(m·K)]	h_{inf}	20 [m]
c	1465 [J/(kg·K)]	h_0	20 [W/(m ² ·K)]
ρ	1588 [kg/m ³]	B	9.0 [K]
\dot{m}_L	0.57 [kg/s]	B_d	5.0 [K]
c_L	3700 [J/(kg·K)]	t_{max}	190 [days]
A_g	450 [m ²]	T_b	9.5 [°C]

The measurement results, together with the results of calculations according to the presented model, are depicted in Figs. 7a and b. The symbols represent the experimental values read out from the drawings shown in [6] referred to the 28th of December. Fig. 7a presents temperature profiles for the ground without a heat exchanger, while Fig. 7b refers to temperature profiles around the working heat exchanger in which the working fluid receives the heat from the ground. As one can see, the predictions based on the model are correct, although there are small difference in temperature determined experimentally and computationally.

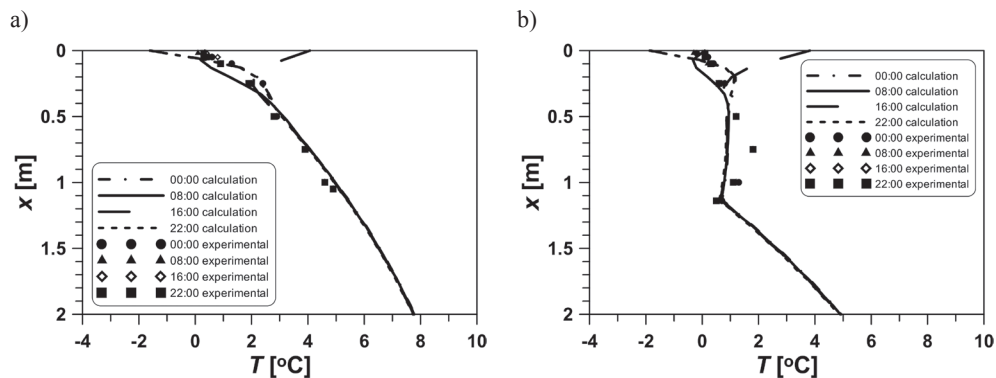


Fig. 7. Comparison of computational and experimental values: a – ground under natural conditions, b – working ground heat exchanger

It should be noted that the compatibility of temperature profiles in Fig. 7a and b depends mainly on the consistency of the actual air temperature in the research (and the preceding) period with the temperature used in the calculations. To generate the data for Fig. 7a, $A_g = 450 \text{ m}^2$ was assumed.

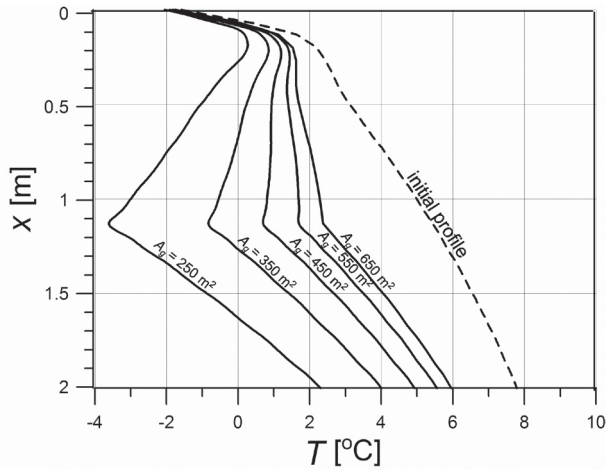


Fig. 8. The effect of the parameter A_g on temperature profiles in the ground

The effect of the adjustable parameter A_g on the temperature profiles in the ground is presented in Fig. 8. The calculations were performed on the basis on the data shown in Table 1. The greater value of A_g the lower the ground temperature drop with respect to initial temperature profile in the ground, determined according to relationship (8). The reason is that the greater value of A_g corresponds to the greater mass of cooled ground. Therefore, the relationship between A_g and the real value (geometric) of the ground area is significant. For a high-density embedded exchanger tubes, the value A_g is close to the geometrical ground area, wherein, the exchanger pipes are installed. For long times of the process duration the amount of A_g might exceed the geometric area (additional heat conduction in horizontal direction). However, the lower packing of tubes along with the shorter time of the heat receiving process from the ground, the more the values of A_g deviate (are smaller) from the geometric area.

For calculations presented in Fig. 7b, the value of A_g is assumed to be approx. 40% higher than the geometric area derived directly from the calculations of the area of trenches dug out for the installation of the heat exchanger pipes: $4 \cdot 1 \cdot 80 = 320 \text{ m}^2$.

5. Conclusions

- The resistance of heat transfer between the surface of the ground and the environment (external thermal resistance of heat transfer) strongly affects the heat flux and the amount of heat, transferred between the ground and the environment as well as the temperature distribution of the sub-surface layer of ground. Reduction of this resistance is beneficial during receiving of heat by the ground exchangers;
- Heat transfer in a horizontal ground heat exchanger can be described by a model based on one-dimensional transient heat conduction equation with an internal heat source;

- The temperature profiles in the ground determined with the use of the presented mathematical model are consistent with the results of the measurements given in literature;
- The presented model can be used to analyze the effects of various process parameters on the ground heat exchanger efficiency.

References

- [1] Demir H., Koyun A., Temir G., *Heat transfer of horizontal parallel pipe ground heat exchanger and experimental verification*, Applied Thermal Engineering, 29, 2009, 224233.
- [2] Florides G., Kalogirou S., *Ground heat exchangers – A review of systems, models and applications*, Renewable Energy, 32, 2007, 2461–2478.
- [3] Gan G., *Dynamic thermal modeling of horizontal ground-source heat pumps*, International Journal of Low-Carbon Technologies, 8, 2013, 95–105.
- [4] Gonzalez R.G., Verhoef A., Vidale P.L., Main B., Gan G., Wu Y., *Interactions between the physical soil environment and a horizontal ground coupled heat pump for a domestic site in the UK*, Renewable Energy, 44, 2012, 141–153.
- [5] Kupiec K., Larwa B., Gwadera M., *Heat transfer in horizontal ground heat exchangers*, Applied Thermal Engineering, 75, 2015, 270–276.
- [6] Wu Y., Gan G., Verhoef A., Vidale P.L., Gonzalez R.G., *Experimental measurement and numerical simulation of horizontal-coupled slinky ground source heat exchangers*, Applied Thermal Engineering, 30, 2010, 2574–2583.
- [7] Carslaw H.S., Jaeger J.C., *Conduction of Heat in Solids*, second ed., Clarendon Press, Oxford 1959, 65–74.